Available online at www.sciencedirect.com
ScienceDirect
Nuclear Physics A 00 (2014) 1–8
Nuclear Physics A

arXiv:1412.0471v1 [hep-ph] 1 Dec 2014

Initial state in relativistic nuclear collisions and Color Glass Condensate

François Gelis

Institut de Physique Théorique, CEA/Saclay, 91191 Gif sur Yvette cedex, France

Abstract

In this talk, I discuss recent works related to the pre-hydrodynamical stages of ultra-relativistic heavy ion collisions.

Keywords: Heavy Ion Collisions, Color Glass Condensate, Initial State

1. Introduction

Hydrodynamical models are very successful at reproducing bulk observables in high energy heavy ion collisions. However, it is a long standing puzzle to understand from the underlying Quantum Chromodynamics (QCD) why this description is so effective. Indeed, the description of the early stages of heavy ion collisions which is most closely related to QCD –the Color Glass Condensate (CGC) framework– predicts at the very beginning of the fireball evolution a situation which is very different from a quasi perfect fluid.

The purpose of this talk is to discuss recent works aiming at a first principles CGC description of the early stages of heavy ion collisions, where by "early stages" we mean the pre-hydrodynamical evolution (left part of fig. 1). Ultimately, the goal is to have a description of these early stages that explains how the hydrodynamical behavior develops and that matches smoothly into hydrodynamics (right part of fig. 1), in such a way that the time τ_0 at which the switching happens becomes unessential (in the same spirit as a factorization scale for parton distributions). Note

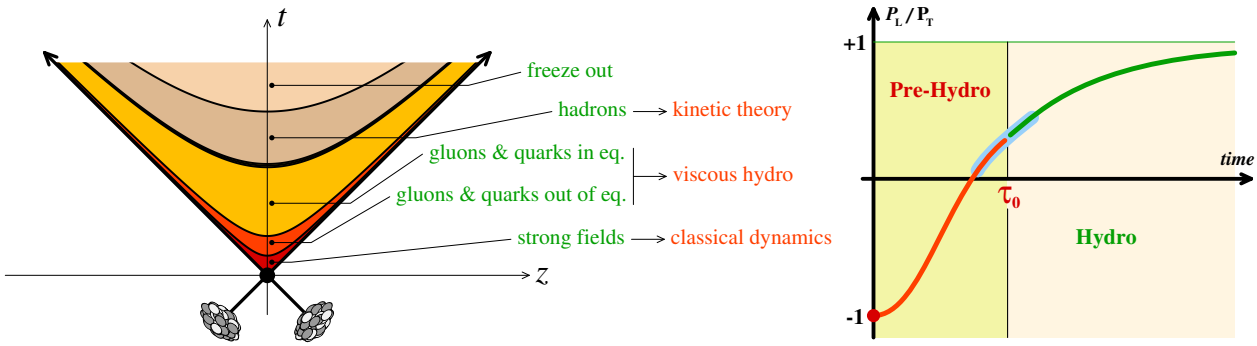


Figure 1. Left: stages of a heavy ion collision. Right: matching to hydrodynamics.

that the CGC, despite being is a weakly coupled framework, can be the siege of strong interactions because the color fields are large, of order g^{-1} (or equivalently the gluon occupation number is of order g^{-2}).

2. Color Glass Condensate

In high energy heavy ion collisions, most particles are produced with a comparatively small transverse momentum of a few GeV at most. Given the longitudinal momentum of the incoming nucleons at the LHC energy, their constituents are probed with a longitudinal momentum fraction $x \lesssim 10^{-3}$, where the gluon distribution is very large (left plot in fig. 2). In this regime of large gluon density, multigluon processes become important, as illustrated in the

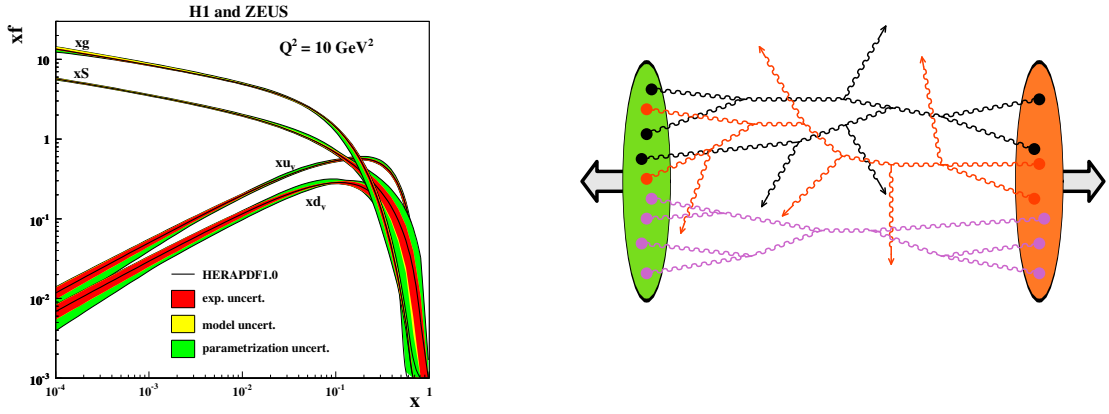


Figure 2. Left: parton distributions in a proton. Right: multiparton scattering at high gluon density.

right panel of the figure 2. These non-linear effects are one of the manifestations of *gluon saturation* [1, 2], which plays a role for transverse momenta $k_\perp^2 \lesssim Q_s^2$, where Q_s is an x-dependent momentum scale known as the saturation momentum (roughly speaking, $\alpha_s^{-2} Q_s^2$ is the gluon density per unit of transverse area, and $\alpha_s^{-2} Q_s^2 / k_\perp^2$ can be viewed as the gluon occupation number). The dependence of Q_s on x and the mass number A is shown in the left plot of fig. 3.

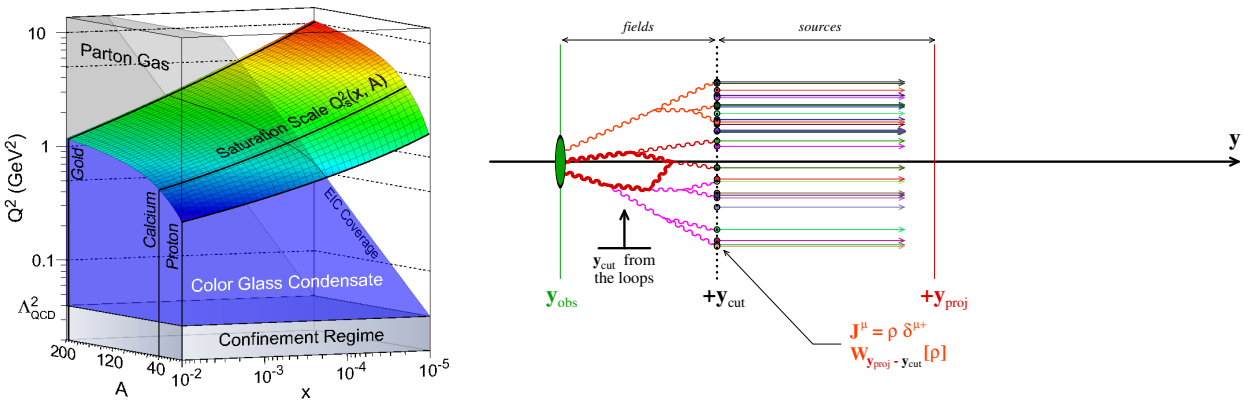


Figure 3. Left: x and A dependence of Q_s (from [3]). Right: high energy factorization in the CGC framework.

In the Color Glass Condensate framework [4–6], the partons that have a longitudinal momentum above a cutoff Λ are treated as a color current $J^\mu = \delta^{\mu+}\rho(\boldsymbol{x}_\perp)$ along the light-cone, while those that have a longitudinal momentum below the cutoff (mostly gluons) are described as usual gauge fields. The transverse color distribution of the fast partons, $\rho(\boldsymbol{x}_\perp)$, fluctuates event-by-event, and the CGC only provides its probability distribution $W[\rho]$. The cutoff Λ separating the two types of degrees of freedom is not a physical parameter, and observables should not depend upon it. This

leads to a renormalization group equation for the distribution $W[\rho]$, known as the JIMWLK equation [7–9] ($W[\rho]$ must depend on Λ in such a way that it cancels the Λ dependence that arises from loop corrections, as illustrated in the right part of fig. 3 – one can show that this dependence is universal for inclusive observables [10, 11]). A recent development is the extension of the JIMWLK equation beyond leading order, with the inclusion of running coupling corrections in ref. [12] and a derivation of the complete NLO result in refs. [13–15].

In practical calculations, the CGC can be viewed as an effective Yang-Mills theory coupled to an external color current $J_1^\mu + J_2^\mu$ (each term corresponding to one projectile). In the saturation regime, these currents are proportional to g^{-1}, and each order in the g^2 expansion is the sum of an infinite set of graphs. At leading order, observables are obtained from the solution of the classical Yang-Mills equations $D_\mu F^{\mu\nu} = J_1^\nu + J_2^\nu$. This solution is known analytically

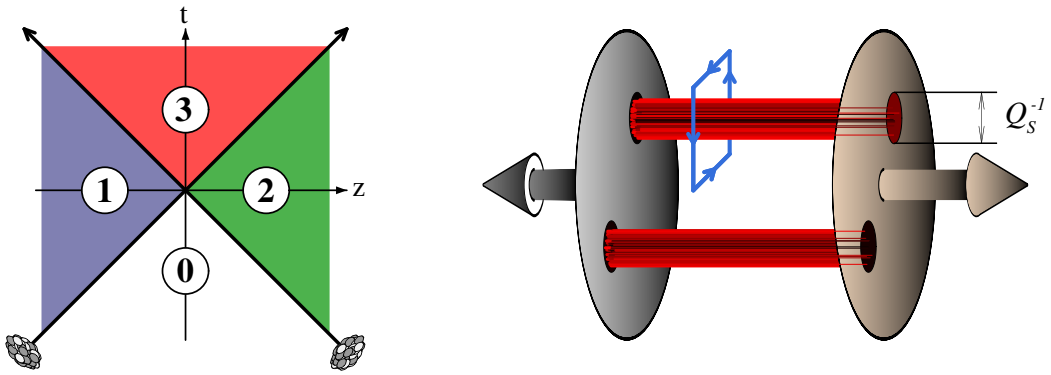


Figure 4. Left: different regions of space-time when solving the Yang-Mills equations. Right: structure of the color field lines just after the collision.

in the regions 0,1,2 of the left plot of fig. 4, but must be obtained numerically [16, 17] in the region 3 (it is known analytically at the interface between 1,2 and 3). Immediately after the collision, the chromo-electric and chromo-magnetic fields are parallel to the collision axis [18] (fig. 4, right), forming longitudinal flux tubes. The typical transverse size of these flux tubes can be assessed by computing the expectation value of Wilson loops $\mathcal{W}$ of varying areas: the observation of an approximate area law, $\mathcal{W} \sim \exp(-\text{const} \times \text{Area})$, for areas above Q_s^{-2}, suggests that the typical transverse size of the flux tubes is Q_s^{-1} [19, 20].

3. Towards hydrodynamical behavior

For hydrodynamics to describe the bulk observables in heavy ion collisions, two conditions must be realized: (i) the ratio of longitudinal to transverse pressure should not be too small (for the stability of hydrodynamical codes) and (ii) the shear viscosity to entropy ratio η/s must be small (for an efficient transfer from spatial to momentum anisotropy, as required by RHIC and LHC data).

In a weakly interacting system, η/s is large. For QCD, it reads [21] $\eta/s \approx 5.1/(g^4 \ln(2.4/g))$ at leading log accuracy. On the other hand, it has been calculated to be $1/4\pi$ in the strong coupling limit of SUSY $N = 4$ Yang-Mills theories [22] (see the plot on the left of fig. 5). Besides this limit, the ratio η/s can also be small at weak coupling provided that the occupation number is large. Generically, η/s is the ratio of the mean free path to the De Broglie wavelength of the constituents. In the CGC, this wavelength is Q_s^{-1}, while the inverse mean free path reads

$$(\text{mean free path})^{-1} \sim \underbrace{g^4 Q^{-2}}_{\text{cross section}} \times \underbrace{\int_{\boldsymbol{k}} f_{\boldsymbol{k}}}_{\text{density}} \underbrace{(1 + f_{\boldsymbol{k}})}_{\substack{\text{Bose} \\ \text{enhancement}}} \quad . \tag{1}$$

When $f_{\boldsymbol{k}} \sim g^{-2}$ (i.e. in the strong field regime prevalent in the CGC), the powers of the coupling cancel and one can evade the conclusion obtained in the weakly interacting scenario.

However, at leading order in the CGC description of heavy ion collisions, the ratio P_L/P_T has a behavior which is quite different from the one expected in hydrodynamics: just after the collision, P_L is exactly opposite to P_T (this

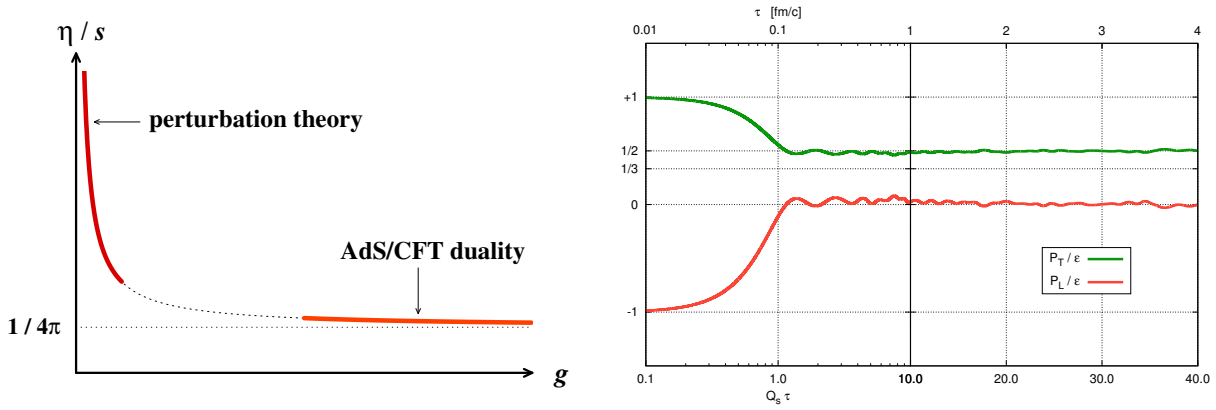


Figure 5. Left: ratio η/s as a function of the coupling. Right: P_L and P_T in the CGC at LO.

is a generic feature of longitudinal $\boldsymbol{E}$ and $\boldsymbol{B}$ fields), and then grows to become mostly positive while remaining much less than P_T at all times, as shown in the right plot of fig. 5. Therefore, the matching[1] from the CGC at LO to

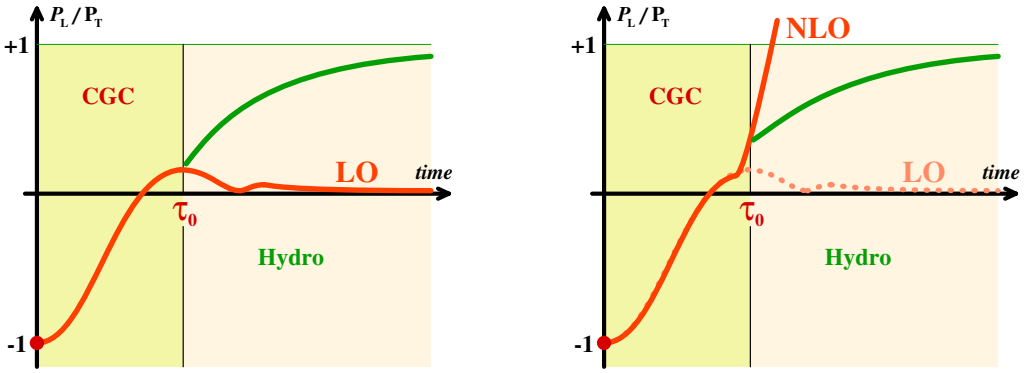


Figure 6. Matching between the CGC and hydrodynamics (Left: LO, Right: NLO).

hydrodynamics is not satisfactory (left part of fig. 6) because the two sides of the matching describe different physics.

The next to leading order CGC result is affected by instabilities in the classical solutions of the Yang-Mills equations: rapidity dependent perturbations grow exponentially with time, and induce a similar behavior in the longitudinal pressure. At NLO, the matching of the CGC to hydrodynamics is still unnatural, as illustrated in the right plot of fig. 6. As shown in the left part of fig. 7, the NLO amounts to a one-loop correction embedded in the classical color fields obtained at LO. This loop has an imaginary part, related to the possibility of gluon pair production by the background field. However, in a strict NLO calculation, there is no feedback from the produced gluons on the background field, which leads to a runaway behavior. This physics has been modeled in a color flux tube model [23], where the produced gluons obey a Boltzmann equation with a source term reflecting their production by the background field (via the Schwinger mechanism in this model), and contribute to an induced color current that feeds back in the Yang-Mills equation that governs the color fields. In this simple model, it is observed that the ratio P_L/P_T approaches 1 when the collision rate is tuned so that $4\pi\eta/s$ is of order one.

In order to study this physics in the CGC framework, one must go beyond fixed order calculations. Indeed, simple power counting arguments suggest that the exponential in time growth seen at NLO becomes even worse at

[1] To match a CGC calculation to hydrodynamics, one should in principle compute the CGC energy-momentum tensor, then find its time-like eigenvector to determine the local flow velocity and energy density. Then, by assuming an equation of state $P = f(\epsilon)$, one get the viscous part of the stress tensor as the difference between the full and the ideal $T^{\mu\nu}$. Note that very often, this procedure is approximated by neglecting the initial flow and the viscous stress.

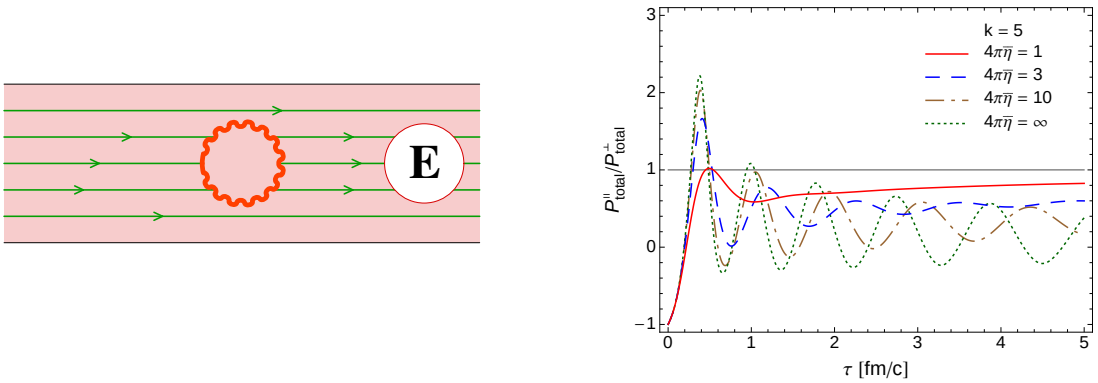


Figure 7. Left: one-loop embedded in a background field. Right: ratio P_L/P_T in the color flux tube model of ref. [23].

higher fixed loop orders. Given the central role played by classical color fields in the CGC, the *classical statistical approximation* (CSA) is a natural extension to achieve such a resummation. In a broad sense, the CSA amounts to performing an average of classical solutions of the field equations over an ensemble of initial conditions. Thanks to the fact that one is solving the fully non-linear equations of motion, the CSA is free of the exponentially growing terms encountered in fixed order calculations (in contrast, the NLO calculation amounts to solving the linearized equations of motion over some background), for any theory where the Hamiltonian is bounded from below. In studies of heavy ion collisions, the CSA is easy to implement, by discretizing the $\boldsymbol{x}_\perp, \eta$ coordinates, as illustrated in the right panel of fig. 8 (contrary to the CGC at LO, it is now necessary to keep the rapidity dependence of the fields because the fluctuations of the initial conditions break the boost invariance of individual field configurations – even though the physics is boost invariant on average).

An important issue when using the CSA is that of the ultraviolet divergences. Roughly speaking, the fluctuations of the initial fields can be categorized in two kinds, vacuum fluctuations and quasiparticle excitations, that can be easily seen in the bare propagator G_{22} of the retarded/advanced formalism,

$$G_{22}(p) \sim \underset{\text{quasiparticles}\ \hookleftarrow}{f_0(\boldsymbol{p})} + \underset{\hookrightarrow\ \text{vacuum fluctuations}}{\frac{1}{2}}\,\delta(p^2)\,. \tag{2}$$

The vacuum fluctuations have a flat spectrum in momentum space, while the fluctuations associated to quasiparticles have a spectrum that fall like the initial distribution $f_0(\boldsymbol{p})$. The quasiparticle-induced fluctuations lead to super-renormalizable contributions [24], provided that $f_0(\boldsymbol{p})$ falls at least as fast as p^{-1}. In contrast, the vacuum fluctuations lead to ultraviolet divergences. Moreover, since the CSA misses some quantum contributions of the full theory, it is non-renormalizable [25], as can be seen by the presence of ultraviolet divergences in self-energies that have no associated operator in the Lagrangian,

$$\text{Im}\ \raisebox{-0.5em}{\includegraphics[height=2.2em]{}} = -\frac{g^4}{1024\pi^3}\left(\Lambda_{\text{UV}}^2 - \frac{2}{3}p^2\right). \tag{3}$$

When initializing the CSA with vacuum fluctuations, one can for instance observe a strong dependence on the ultraviolet cutoff of the state reached by the system at late times, as shown in the plot [26] on the right of fig. 8. It appears that this sensitivity can be minimized when the UV cutoff is in the range $3-6$ times the physical scale, but one should keep in mind when using this type of initial conditions that the lack of renormalizability prevents a proper continuum limit.

In the limit where the ensemble of initial conditions narrows down to a delta function, one recovers the CGC LO result. It can be shown that there exists a unique Gaussian ensemble of initial conditions such that the CSA reproduces the exact LO and NLO results, plus a subset of all higher order terms. This Gaussian ensemble, that can be determined analytically at $Q_s\tau \ll 1$ [27], is centered on the LO classical field, and its variance is obtained by solving the linearized

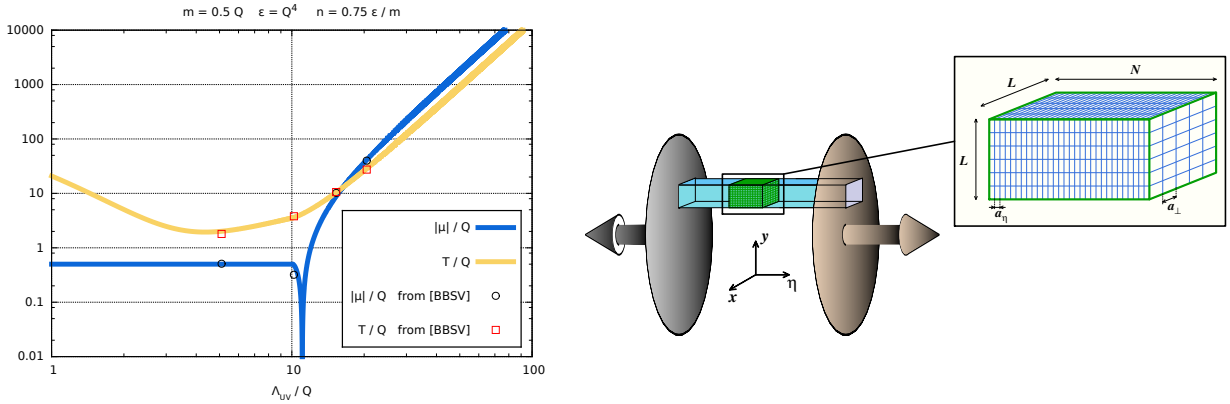


Figure 8. Left: dependence on the UV cutoff of the temperature and chemical potential at late times. Right: lattice setup for simulating heavy ion collisions in the CSA.

Yang-Mills equations over the LO background, with a plane wave initial condition in the remote past (left of fig. 9) :

$$\langle \mathcal{A}^\mu \rangle = \mathcal{A}^\mu_{\rm LO} \qquad \text{Variance} = \int_{\text{modes } \boldsymbol{k}} \frac{1}{2}\, a_{\boldsymbol{k}}(\boldsymbol{u}) a^*_{\boldsymbol{k}}(\boldsymbol{v}) \qquad \Big[\mathcal{D}_\rho \mathcal{D}^\rho \delta^\nu_\mu - \mathcal{D}_\mu \mathcal{D}^\nu + ig\,\mathcal{F}_\mu{}^\nu\Big] a^\mu_{\boldsymbol{k}} = 0 \qquad \lim_{x^0 \to -\infty} a_{\boldsymbol{k}}(x) = e^{ik\cdot x} \tag{4}$$

However, these initial conditions are (dressed) vacuum fluctuations, and therefore lead to a non-renormalizable CSA. Other works [28, 29] have considered a particle-like Gaussian ensemble of initial fluctuations, with a vanishing central

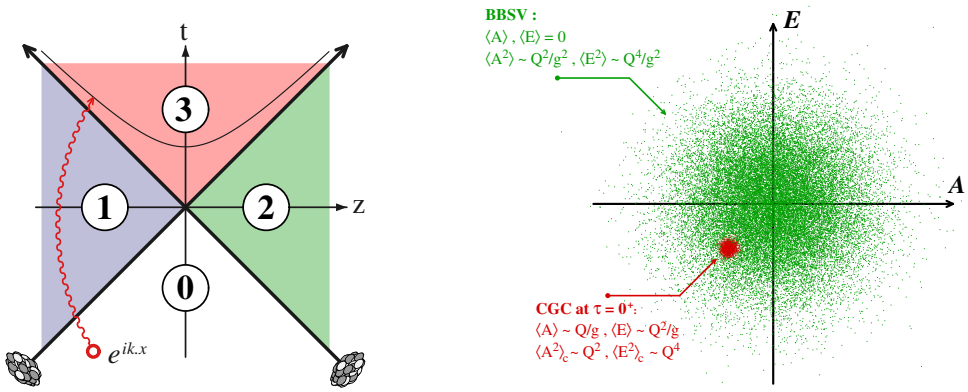


Figure 9. Left: calculation of the initial CGC fluctuations. Right: phase-space distributions in two implementations of the CSA.

value and large fluctuations :

$$\langle \mathcal{A}^\mu \rangle = 0 \qquad \text{Variance} = \int_{\text{modes } \boldsymbol{k}} f_0(\boldsymbol{k})\, a_{\boldsymbol{k}}(\boldsymbol{u}) a^*_{\boldsymbol{k}}(\boldsymbol{v}) \qquad a_{\boldsymbol{k}}(x) \equiv e^{ik\cdot x} \qquad f_0(\boldsymbol{k}) \sim g^{-2} \times \theta(Q_s - k) \tag{5}$$

These initial conditions lead to a proper UV limit, but whether they can be connected with CGC fields at $Q_s\tau \ll 1$ is unclear at the moment. In this model, one can play with the gluon distribution $f_0(\boldsymbol{k})$ in order to control the magnitude of the initial occupancy and its anisotropy in momentum space. The difference between the initial conditions of type (4) and (5) is illustrated in the plot on the right of fig. 9.

Some results obtained with these two types of initial conditions are shown in the figure 10 (Left: CGC initial conditions at $Q_s\tau \ll 1$, Right: particle-like initial conditions at $Q_s\tau \gg 1$). With CGC vacuum-like fluctuations, the ratio P_L/P_T is found to increase significantly above the LO values, for a coupling $g = 0.5$ [30]. However, one

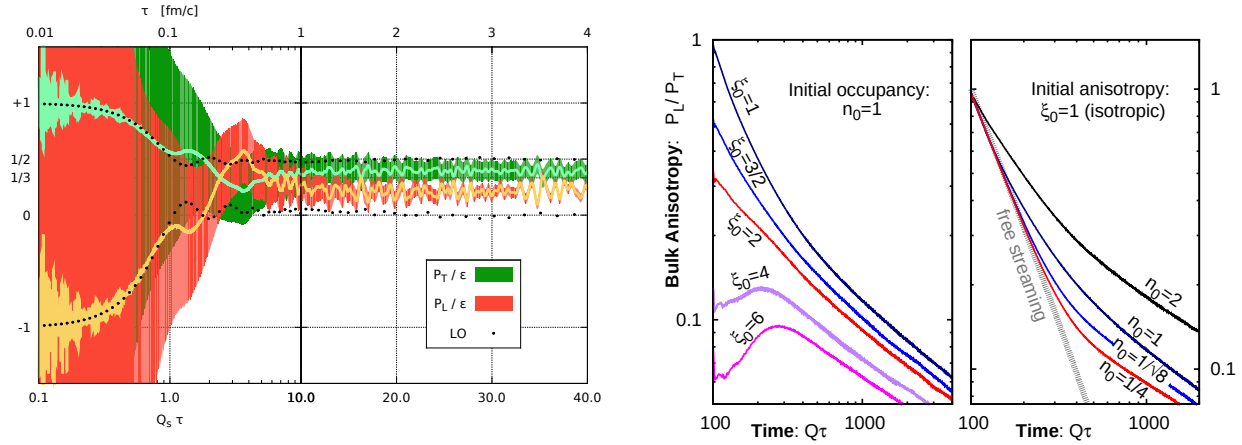


Figure 10. Results of the CSA for the ratio P_L/P_T. Left : CGC vacuum-like initial fluctuations at $Q_s\tau \ll 1$ [30]. Right : particle-like initial fluctuations at $Q_s\tau \gg 1$ [28, 29].

should keep in mind that this calculation was performed on a small lattice ($64 \times 64 \times 128$) and that because the initial conditions are vacuum fluctuations it has no continuum limit. With particle-like initial fluctuations, and starting at a much larger time, the study of ref. [28, 29] found a ratio P_L/P_T that reaches a universal behavior for varying initial occupations and anisotropies, following a self-similar evolution

$$f(t, p_\perp, p_z) \sim \tau^{-2/3}\, f_s(\tau^0 p_\perp, \tau^{1/3} p_z) \qquad \frac{P_L}{P_T} \sim \tau^{-2/3} \tag{6}$$

intermediate between free streaming,

$$f(t, p_\perp, p_z) \sim \tau^{0}\, f_s(\tau^0 p_\perp, \tau^{1} p_z) \qquad \frac{P_L}{P_T} \sim \tau^{-2}\,, \tag{7}$$

and expansion at constant anisotropy :

$$f(t, p_\perp, p_z) \sim \tau^{\frac{2(\delta-1)}{2+\delta}}\, f_s(\tau^{\frac{\delta}{2+\delta}} p_\perp, \tau^{\frac{\delta}{2+\delta}} p_z) \qquad \frac{P_L}{P_T} = \delta\,. \tag{8}$$

With this kind of initial conditions, the coupling constant g cancels out and does not affect the time dependence of P_L/P_T. The coupling only affects the time at which the fields (that decrease with time) become too small for the classical approximation to be trusted, since they start with a magnitude $\sim g^{-1}$. When this happens, one should switch to a description that has quantum effects built in. In the case of non-expanding systems, classical statistical simulations have been combined with an effective kinetic theory description that takes over the evolution of the system at low occupation numbers, in order to follow the time evolution of the system from a highly occupied initial condition all the way to thermal equilibrium [31–33].

Let us finish this overview by mentioning some works on Bose-Einstein condensation (BEC), that has been speculated to occur in heavy ion collisions due to the initially overoccupied gluon distribution. The starting observation is that in the CGC, the dimensionless ratio $n/\epsilon^{3/4}$ (n being the number of gluons per unit volume) is initially $g^{-1/2}$ and is thus large at weak coupling, while it is of order unity in thermal equilibrium [34]. To resolve this discrepancy, the system can eliminate the excess of gluons via inelastic processes (e.g. $3 \to 2$), or by forming a condensate at $k = 0$ (at asymptotic times, this BEC should disappear because the gluon number is not conserved). The formation of such a condensate has been observed in scalar theories studied in the classical statistical approximation [35, 36]. In QCD, kinetic theory computations do see the formation of a BEC [37], even if only as a transient phenomenon when number changing processes are included, while other calculations show no sign of it [31, 32]. Even if such a condensate would form, its phenomenological consequences are unclear at the moment. Rather intriguingly, fits of pion spectra at very low momentum [38] tend to support a positive chemical potential almost equal to the pion mass, which is the value that would be realized if a transient pion condensate was formed.

4. Conclusions

The CGC provides a QCD-based theoretical framework for studying from first principles the initial stages of heavy ion collisions. The parton content of the colliding projectiles is represented in the form of probability distributions $W[\rho]$ for the color charge transverse density. These distributions obey a universal RG equation –the JIMWLK equation– which is now known up to NLO, and enter into factorized expressions for all inclusive observables.

At early times after the collision of two heavy ions, the CGC can be viewed as a weakly coupled (because the relevant momentum scale is the saturation momentum $Q_s \gg \Lambda_{\rm QCD}$, that increases with the collision energy), but strongly interacting system (because it contains color fields that are of order g^{-1}).

Fixed order calculations do not match properly onto the expected hydrodynamical behavior. At LO, the longitudinal pressure never becomes comparable to the transverse one, while at NLO instabilities make it increase indefinitely in an unphysical way. One can go beyond this by using the classical statistical method, where one solves classical field equations with fluctuating initial conditions. At the moment, two recent works have implemented it with two different types of initial conditions, leading to different results regarding the isotropization of the pressure tensor.

Acknowledgements : This work is supported by the Agence Nationale de la Recherche project 11-BS04-015-01.

References

[1] L.V. Gribov, E.M. Levin, M.G. Ryskin, Phys. Rept. **100**, 1 (1983).
[2] A.H. Mueller, J-W. Qiu, Nucl. Phys. **B 268**, 427 (1986).
[3] A. Deshpande, R. Ent, R. Milner, CERN Courier, October 2009.
[4] L.D. McLerran, R. Venugopalan, Phys. Rev. **D 49**, 2233 (1994).
[5] L.D. McLerran, R. Venugopalan, Phys. Rev. **D 49**, 3352 (1994).
[6] F. Gelis, E. Iancu, J. Jalilian-Marian, R. Venugopalan, Ann. Rev. Part. Nucl. Sci. **60**, 463 (2010).
[7] I. Balitsky, Nucl. Phys. **B 463**, 99 (1996).
[8] E. Iancu, A. Leonidov, L.D. McLerran, Nucl. Phys. **A 692**, 583 (2001).
[9] E. Iancu, A. Leonidov, L.D. McLerran, Phys. Lett. **B 510**, 133 (2001).
[10] F. Gelis, T. Lappi, R. Venugopalan, Phys. Rev. **D 78**, 054019 (2008).
[11] F. Gelis, T. Lappi, R. Venugopalan, Phys. Rev. **D 78**, 054020 (2008).
[12] T. Lappi, H. Mäntysaari, Eur. Phys. J. **C 73**, 2307 (2013).
[13] A.V. Grabovsky, JHEP **1309**, 141 (2013).
[14] A. Kovner, M. Lublinsky, Y. Mulian, Phys. Rev. **D 89**, 061704 (2014).
[15] A. Kovner, M. Lublinsky, Y. Mulian, arXiv:1405.0418.
[16] A. Krasnitz, R. Venugopalan, Phys. Rev. Lett. **84**, 4309 (2000).
[17] T. Lappi, Phys. Rev. **C 67**, 054903 (2003).
[18] T. Lappi, L.D. McLerran, Nucl. Phys. **A 772**, 200 (2006).
[19] A. Dumitru, Y. Nara, E. Petreska, Phys. Rev. **D 88**, 054016 (2013).
[20] A. Dumitru, T. Lappi, Y. Nara, Phys. Lett. **B 734**, 7 (2014).
[21] P. Arnold, G.D. Moore, L.G. Yaffe, JHEP **0011**, 001 (2000).
[22] G. Policastro, D.T. Son, A.O. Starinets, Phys. Rev. Lett. **87**, 081601 (2001).
[23] R. Ryblewski, W. Florkowski, Phys. Rev. **D 88**, 034028 (2013).
[24] G. Aarts, J. Smit, Phys. Lett. **B 393**, 395 (1997).
[25] T. Epelbaum, F. Gelis, B. Wu, arXiv:1402.0115.
[26] J. Berges, K. Boguslavski, S. Schlichting, R. Venugopalan, JHEP **1405**, 054 (2014).
[27] T. Epelbaum, F. Gelis, Phys. Rev. **D 88**, 085015 (2013).
[28] J. Berges, K. Boguslavski, S. Schlichting, R. Venugopalan, Phys. Rev. **D 89**, 074011 (2014).
[29] J. Berges, K. Boguslavski, S. Schlichting, R. Venugopalan, Phys. Rev. **D 89**, 114007 (2014).
[30] T. Epelbaum, F. Gelis, Phys. Rev. Lett. **111**, 232301 (2013).
[31] A. Kurkela, G.D. Moore, Phys. Rev. **D 86**, 056008 (2012).
[32] M.C. Abraao York, A. Kurkela, E. Lu, G.D. Moore, Phys. Rev. **D 89**, 074036 (2014).
[33] A. Kurkela, E. Lu, arXiv:1405.6318.
[34] J.P. Blaizot, F. Gelis, J. Liao, L. McLerran, R. Venugopalan, Nucl. Phys. **A 873**, 68 (2012).
[35] T. Epelbaum, F. Gelis, Nucl. Phys. **A 872**, 210 (2011).
[36] J. Berges, D. Sexty, Phys. Rev. Lett. **108**, 161601 (2012).
[37] J.P. Blaizot, J. Liao, L.D. McLerran, Nucl. Phys. **A 920**, 58 (2013).
[38] V. Begun, W. Florkowski, M. Rybczynski, Phys. Rev. **C 90**, 014906 (2014).